ARTICLE TYPE

A General Approach toward Polymer-Coated Plasmonic Nanostructures

Marek Grzelczak,*[a,b] Ana Sánchez-Iglesias[a] and Luis M. Liz-Marzán[a,b,c]

5 **We report a generic method for the preparation of polymer-coated plasmonic nanostructures with tunable thickness of the hydrophobic polymer spacer. By simply changing the order of addition of a block copolymer and water, encapsulation of either individual or assembled nanoparticles** 10 **within copolymer micelles can be selected, thus providing wide versatility to the method.**

Combination of nanoparticles (NPs) and polymers in colloidal phase provides unique chemical tools toward the development of multifunctional platforms with properties that are characteristic of 15 both components - e.g. hard inorganic core and soft polymer shell.[1] While inorganic cores provide interesting physical properties (light absorption, scattering or emission, magnetic response, etc.), the polymeric chains exhibit chemically relevant characteristics, so their combination may be of importance in 20 both life science and materials science. One of the most versatile strategies for the synthesis of polymer-coated NPs is based on the encapsulation of alkyl chain-stabilized nanoparticles with amphiphilic polymers.[2] In this strategy, the polymer acts as a surfactant allowing the transfer of hydrophobic nanoparticles 25 from non-polar into polar solvents (*organic-to-water*). This method, however, is usually limited to the encapsulation of small and isotropic nanoparticles, since large and non-spherical nanoparticles have proven difficult to be stabilized by small alkyl chains, which are often used in organic NP synthesis. Phase 30 transfer processes are often difficult to control and still rather unpredictable.

Morphologically diverse plasmonic NPs with interesting optical properties are frequently synthesised in water, in the presence of surfactants. Subsequent functionalization with 35 polyelectrolytes,[3] or other functional polymers such as polyvinylpyrrolidone[4] can be performed after synthesis but a fraction of surfactant molecules may remain, eventually resulting in polymer detachment. Therefore, a more convenient way comprises the transfer of the NPs from water to an organic 40 solvent via ligand exchange, followed by transfer back to aqueous solution via polymer encapsulation (*water-to-organic-to-water*). The transfer of NPs from water to organic solvents is in fact experimentally challenging, since short alkanethiols are unable to stabilize non-spherical nanoparticles with dimensions above 100 45 nm. Recently, bidentated thiol ligands (oleyl derivatives),[5] thiol-terminated polystyrene,[6,7] or block copolymers[8,9] have been used to efficiently disperse anisotropic NPs in organic solvents.

On the other hand, polymer-stabilized NPs in organic solvents offer a great chemical playground for directed self-assembly,[10–13] 50 simply by changing solvent composition.[14–16] Importantly, amphiphilic polymers have been used to encapsulate NP assemblies and stabilize them in water, thus expanding their applications.[17–24] Notwithstanding, generic experimental methods are still required for the encapsulation of individual plasmonic 55 nanoparticles with various shapes, as well as plasmonic NP assemblies. We show here that this can be achieved by using an amphiphilic block copolymer (polystyrene – diblock –polyacrylic acid, or PS-*b*-PAA), as schematically shown in **Fig. 1**. We first demonstrate the successful transfer of water-stable, nanospheres, 60 nanorods and nanostars into tetrahydrofuran (THF), via ligand exchange of the native CTAB surfactant with thiolated polystyrene (PS). Subsequent addition of water to the mixture containing PS-stabilized NPs (Au@PS) and PS-b-PAA leads to the encapsulation of individual NPs by hydrophobic interactions 65 between polystyrene grafted on the nanoparticles surface and the PS block of the copolymer. On the contrary, when water is added to Au@PS in THF, the NPs gradually aggregate into organized assemblies, again via hydrophobic interactions, which can then be stabilized through subsequent addition of PS-b-PAA. Thus, by 70 simply changing the order of addition of block copolymer and water, we can select either the encapsulation of individual NPs or of their assemblies. This method is particularly simple because water and THF are miscible and thus the particles are not required to cross through a liquid-liquid interface, as in most 75 other methods.[5,25]

The starting gold nanoparticles with three different morphologies - spheres,[26] rods[27] and stars,[28] - were prepared following optimized recipes, and were all stabilized with the cationic surfactant cetyltrimethylammonium bromide (CTAB). 80 We aimed at varying the shape of the particles while keeping their dimensions within the same range: nanospheres (69.5 ± 3.5 nm diameter); nanorods: (70.5 ± 3.5 nm length; 12.3 ± 1.3 nm width; aspect ratio 3.5); nanostars: (55.8 ± 7.0 nm core diameter; 38.2 ± 9.1 nm tip length). It has been reported that the shape of 85 the NPs determines the spatial distribution of grafted polymer, likely due to changes in curvature.[6] Thus, CTAB was used as the common initial stabilizer, to ensure that only the shape of the particles can affect the ligand exchange process. CTAB molecules were removed as previously reported[17] to graft thiol-90 terminated polystyrene (PS, Mw = 53,000 g/mol), using an excess of polymer molecules (5 molecules per nm^2). Stable colloidal dispersions of Au@PS were stored in THF, prior to encapsulation experiments by addition of water (10 wt%). To encapsulate

individual nanoparticles, water was added to a mixture of Au@PS and PS-*b*-PAA, whereas encapsulation of NP clusters comprised water addition followed by PS-*b*-PAA after 10 min.
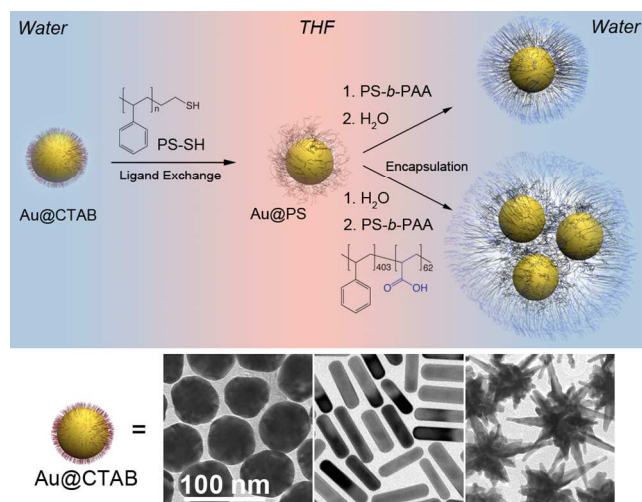
⁵ **Fig. 1** Upper panel: Schematic representation of the strategy for polymer encapsulation of CTAB-stabilized plasmonic nanoparticles and assemblies. Lower panel: Representative TEM micrographs of the gold nanoparticles used in this study: nanospheres, nanorods and nanostars.

In both approaches, the amount of water was subsequently ¹⁰ increased up to 50 wt% to promote hydrophobic forces between polystyrene molecules, thereby increasing the rigidity of the hydrophobic core.[14] Incubation at 70 ℃ for 30 min and subsequent centrifugation helps to expel solvent molecules remaining in the hydrophobic core and to remove free block ¹⁵ copolymer micelles, respectively. The so encapsulated nanoparticles can be easily dispersed in pure water since the outer layer consists of the hydrophilic PAA blocks.

Since water is the most suitable solvent for both the initial (CTAB-stabilized), and the final nanostructures stabilized with ²⁰ PS-*b*-PAA, we carried out all morphological and optical characterizations in aqueous solutions. As shown in **Fig. 2**, the thickness of the polymer shell on spherical nanoparticles is controlled by the molecular weight of the grafted polystyrene. With increasing M_w from 5.8k to 21.5k and 53k, the ²⁵ hydrodynamic diameter, obtained by dynamic light scattering (DLS), increases from 97.0±0.9 nm to 115.3±2.21 nm and 128.9±0.8 nm, respectively, indicating shell thicknesses of 13, 23 and 30 nm (**Fig. 2d**). Although we see a direct relationship between the M_w of grafted PS and shell thickness, the changes in ³⁰ shell thickness might also be related to the enhanced incorporation of copolymer molecules for higher M_w PS. The hydrophobic interaction potential between polymer chains is proportional to M_w, which in this case could lead to attraction of a larger number of copolymer molecules,[17] thereby increasing shell ³⁵ thickness. Regardless of the mechanism of shell formation, we can state that simply by changing the grafted polymer chain length, the final shell thickness can be readily tuned. Such a control over the thickness of the hydrophobic spacer is important toward the design of platforms that can be loaded with small ⁴⁰ cargo molecules/NPs, such us drugs, magnetic nanoparticles or quantum dots.

The thickness of the shell was found to affect the localized surface plasmon resonance (LSPR) of the resulting core-shell nanoparticles. With increasing shell thickness the surface ⁴⁵ plasmon band red-shifts, up to 26 nm for the thickest shell (**Fig. 2d,e**) The origin of this shift is the increased local refractive index around the NPs.[29] Thus, the compact copolymer micelles on the Au@PS surface has thus a similar effect as other transparent shells such as silica[30] or cross-linked pNIPAM.[31]
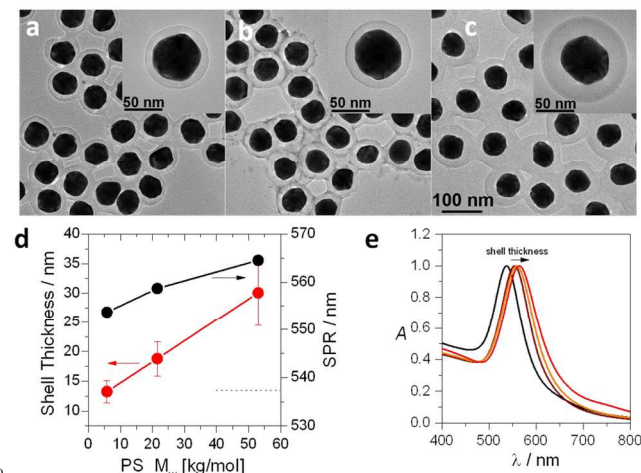
Fig. 2 (a-c) TEM images of spherical Au nanoparticles encapsulated in polymer shells with increasing PS M_w. (d) Shell thickness determined from DLS measurements and LSPR shift versus Mw of grafted polystyrene. (e) Normalized UV-Vis spectra of CTAB-stabilized ⁵⁵ nanoparticles (black) and encapsulated nanoparticles with increasing PS M_w. The solvent is water in all cases.

Encapsulation of individual non-spherical NPs - nanorods and nanostars - proved to be more challenging as compared to ⁶⁰ spherical NPs. We found that PS-*b*-PAA encapsulation of polystyrene chains with lower M_w (5.8k and 21.5k) did not provide sufficient stability in water, so that aggregation occurred upon transfer into water. In contrast to spherical particles, PS is unevenly distributed on the surface of anisotropic NPs, with ⁶⁵ higher grafting density on the areas with higher curvature. In fact, it has been indirectly shown that for gold nanorods[6] or dumbbells[14] polystyrene distributes mostly on the tips, leaving the central part of the particles coated with native CTAB. A large hydrophobic corona expanding over the whole particle surface ⁷⁰ however ensures colloidal stability of the nanorods in THF. Successful encapsulation of individual nanorods within block copolymer micelles thus requires PS with higher M_w, which in this case was found to be 53 kg/mol. Interestingly, TEM observation (**Fig. 3a**) suggests that encapsulation of nanorods ⁷⁵ leads to formation of nearly spherical shells (total hydrodynamic diameter = 97.5±1.3 nm). Therefore, the shell thickness is curvature dependent, ca. 40 nm on the lateral sides, but only 12 nm on the tips. Such a difference in shell thickness stems from minimization of surface area during shell formation. In the TEM ⁸⁰ images, the encapsulated rods appear to be more polydisperse than the initial ones (c.f. **Figs. 1** and **3a**), but this is an optical effect from the random orientation of the nanorods within spherical shells, with different tilting angles on the TEM grid.

During the encapsulation of individual nanostars, the ⁸⁵ copolymer micelles show a tendency to form the most favorable

spherical shape, leading to core-shell structures from which the longer tips protrude out of the copolymer shell (**Fig. 3b**). High resolution TEM images before and after encapsulation suggest that the polymer shell gets adapted to the morphology of the nanoparticle core (**Fig. 3d**). Individual tips of CTAB-stabilized nanostars are covered with a uniform thin layer of organic matter - surfactant adsorbed on the metal.
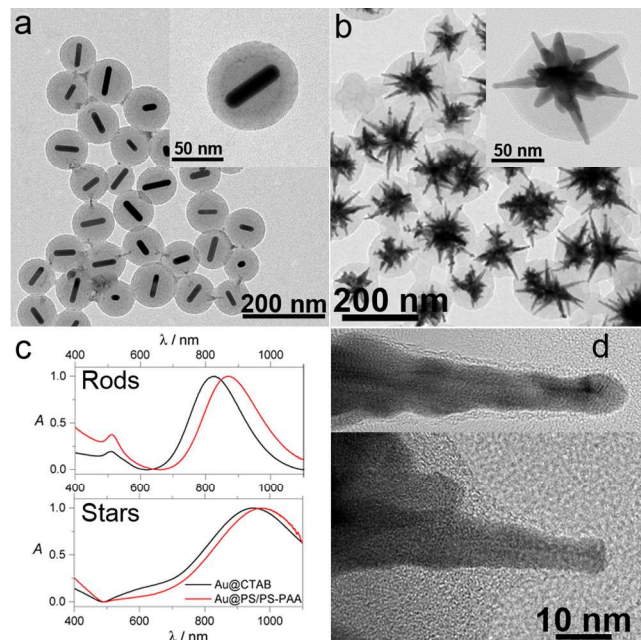
Fig. 3 (a,b) Representative TEM images of polymer encapsulated Au nanorods (a) and nanostars (b). (c) UV-Vis spectra in water of nanorods and nanostars before and after encapsulation. (d) HRTEM images of individual tips in a CTAB-stabilized nanostar (upper panel) and after encapsulation with block copolymer (lower panel), the latter showing webbed soft organic matter on both sides of the tip.

On the other hand, the polymer micelles form a webbed structure between gold tips, suggesting the preferential binding of polystyrene on the lateral parts of the tips rather than on its ends. This intriguing core-shell morphology with partially naked tips may offer an attractive architecture when designing plasmonic biosensors or building blocks for self-assembly e.g. via thiol chemistry. The measured optical properties of the encapsulated nanorods and nanostars are consistent with the observed morphologies. As in the case of encapsulated spheres, the presence of the organic shell on both nanorods and nanostars leads to significant LSPR red-shifts (**Fig. 3c**). For gold nanorods the longitudinal LSPR was found to redshift by 45 nm, while the transverse LSPR shifts by only 3 nm. For nanostars, the tip mode redshifts by 23 nm. Although a longer shift could be expected for nanostars,[32] the effect is probably damped by the partial coverage of the tips with the polymeric shell.

Colloidal stability of Au@PS in pure THF is ensured by steric repulsion, which overcomes attractive van der Waals forces. The presence of water however, partly replaces THF molecules at the polymer/solvent interface, thereby inducing dominating hydrophobic forces that are manifested through an aggregation process. TEM images of the aggregating nanoparticles, 10 min after water addition, revealed disk-like structures regardless of particle shape (**Fig. S1, SI**), as previously reported for spheres.[17]

We assume that the particles aggregate into globular structures, which upon drying on the TEM grids adapt to the flat substrate, forming the observed disk-like structures. Addition of PS-b-PAA to the mixture of aggregating nanoparticles inhibits further aggregation, by dominating hydrophobic interactions between the PS blocks of the copolymer and grafted PS on the nanoparticles surface. Formation of rigid spherical clusters for all particle shapes was achieved at higher water concentration (50 wt%) and thermal treatment (70 ºC) as shown in **Fig. 4**. The diameters of the encapsulated clusters were of the same order: 324.9±34.5 nm, 249.6±43.1 nm, and 252.5±44.8 nm for clusters containing spheres, nanorods and nanostars, respectively. Interestingly, in the interior of the micelles, the nanoparticles adapt to the confined (hydrophobic) space, thereby minimizing inter-particle distances, as previously reported for nanodumbbells.[14]
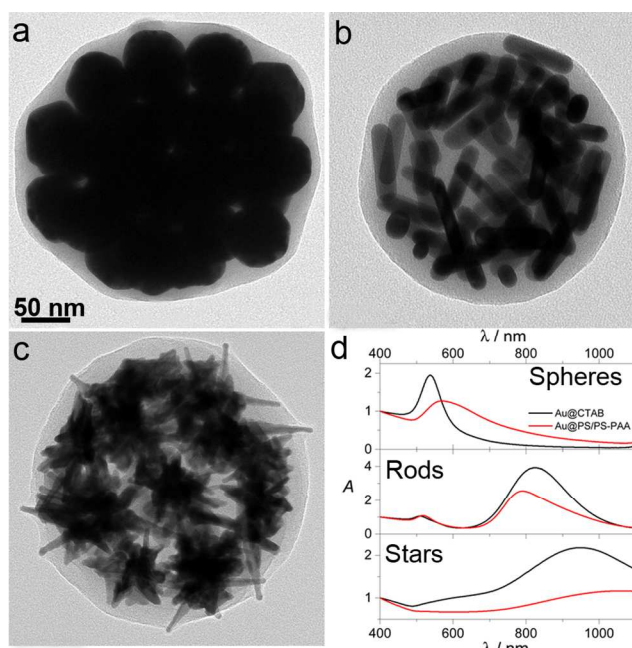
Fig. 4 (a-c) TEM images of single polymer micelles carrying clusters of spheres (a), nanorods (b) and nanostars (c). (d) UV-Vis spectra of the corresponding colloids of encapsulated clusters, showing the LSPR shifts derived from encapsulation. Black lines: CTAB-stabilized NPs; Red lines: encapsulated clusters.

The mutual orientations between NPs depend on their shape. Although conventional TEM analysis is unable to reveal the precise NP distribution, UV-Vis analysis can be used as a complementary tool to understand NP organization. For the clusters containing nanospheres and nanostars, the LSPR peaks were found to redshift by 34 and 111 nm, respectively (**Fig. 4d**). In this case, the LSPR shift originates mainly from plasmon coupling, which is more pronounced in the case of the clusters containing nanostars because of interdigitation of the tips and the resulting enhanced LSPR coupling and hotspot formation. On the other hand, the longitudinal LSPR of clusters containing nanorods is found to blueshift by 34 nm, whereas the transverse LSPR redshifts by 9 nm (**Fig. 4d**). Indeed, it has been shown that plasmon coupling in the side-to-side orientation of gold nanorods leads to longitudinal LSPR blueshift and transverse LSPR redshift. In this case, the LSPR changes are due to a favored side-to-side conformation within the nanorod clusters, as compared to

tip-to-tip or tip-to-side conformations.[33]

Conclusions

We have shown that encapsulation of plasmonic nanoparticles within polymeric micelles leads to formation of spherical systems, regardless of the initial shape of the nanoparticles. To successfully form compact polymeric shells no phase transfer between two immiscible solvents was necessary. The only requirement is the use of miscible solvents with different polarities (THF/water) to stabilize either single particles or clusters thereof in an organic medium and subsequently transfer them to water. We envisage that our general approach is an attractive strategy toward the fabrication of heterogeneous nanostructures based on plasmonic platforms and functional cargo (*e.g.* drug molecules, quantum dots, magnetic nanoparticles) located within the hydrophobic spacer.

Acknowledgements

Notes and references

a Bionanoplasmonics Laboratory, CIC biomaGUNE, Paseo de Miramón 182, 20009 Donostia, San Sebastián, Spain; b Ikerbasque, Basque Foundation for Science, 48011 Bilbao, Spain; c College of Science, King Saud University, P.O.Box 2455, Riyadh 11451, Saudi Arabia

† Electronic Supplementary Information (ESI) available: Detailed experimental part, TEM images of NPs aggregates before encapsulation. See DOI: 10.1039/b000000x/

1. B. Gao, M. J. Rozin, and A. R. Tao, *Nanoscale*, 2013, **5**, 5677–5691.
2. F. Zhang, E. Lees, F. Amin, P. Rivera_Gil, F. Yang, P. Mulvaney, and W. J. Parak, *Small*, 2011, **7**, 3113–3127.
3. A. Gole and C. J. Murphy, *Chem. Mater.*, 2005, **17**, 1325–1330.
4. E. Carbó-Argibay, B. Rodríguez-González, J. Pacifico, I. Pastoriza-Santos, J. Pérez-Juste, and L. M. Liz-Marzán, *Angew. Chem. Int. Ed.*, 2007, **46**, 8983–8987.
5. M. Lista, D. Z. Liu, and P. Mulvaney, *Langmuir*, 2014, **30**, 1932–1938.
6. Z. Nie, D. Fava, E. Kumacheva, S. Zou, G. C. Walker, and M. Rubinstein, *Nat Mater*, 2007, **6**, 609–614.
7. R. J. Hickey, X. Meng, P. Zhang, and S.-J. Park, *ACS Nano*, 2013, **7**, 5824–5833.
8. J. He, Y. Liu, T. Babu, Z. Wei, and Z. Nie, *J. Am. Chem. Soc.*, 2012, **134**, 11342–11345.
9. P. Huang, J. Lin, W. Li, P. Rong, Z. Wang, S. Wang, X. Wang, X. Sun, M. Aronova, G. Niu, R. D. Leapman, Z. Nie, and X. Chen, *Angew. Chem. Int. Ed.*, 2013, **52**, 13958–13964.
10. A. Klinkova, R. M. Choueiri, and E. Kumacheva, *Chem. Soc. Rev.*, 2014, Advance Article.
11. S.-Y. Zhang, M. D. Regulacio, and M.-Y. Han, *Chem. Soc. Rev.*, 2014, **43**, 2301–2323.
12. K. Liu, N. Zhao, and E. Kumacheva, *Chem. Soc. Rev.*, 2011, **40**, 656–671.
13. M. Grzelczak, J. Vermant, E. M. Furst, and L. M. Liz-Marzán, *ACS Nano*, 2010, **4**, 3591–3605.
14. M. Grzelczak, A. Sánchez-Iglesias, H. H. Mezerji, S. Bals, J. Pérez-Juste, and L. M. Liz-Marzán, *Nano Lett.*, 2012, **12**, 4380–4384.
15. W. Li, P. Zhang, M. Dai, J. He, T. Babu, Y.-L. Xu, R. Deng, R. Liang, M.-H. Lu, Z. Nie, and J. Zhu, *Macromolecules*, 2013, **46**, 2241–2248.
16. J. Xu, H. Wang, C. Liu, Y. Yang, T. Chen, Y. Wang, F. Wang, X. Liu, B. Xing, and H. Chen, *J. Am. Chem. Soc*, 2010, **132**, 11920–11922.
17. A. Sánchez-Iglesias, M. Grzelczak, T. Altantzis, B. Goris, J. Pérez-Juste, S. Bals, G. Van Tendeloo, S. H. Donaldson, B. F. Chmelka, J. N. Israelachvili, and L. M. Liz-Marzán, *ACS Nano*, 2012, **6**, 11059–11065.
18. W. Li, S. Liu, R. Deng, J. Wang, Z. Nie, and J. Zhu, *Macromolecules*, 2013, **46**, 2282–2291.
19. W. Li, S. Liu, R. Deng, and J. Zhu, *Angew. Chem. Int. Ed.*, 2011, **50**, 5865–5868.
20. S. G. Jang, E. J. Kramer, and C. J. Hawker, *J. Am. Chem. Soc.*, 2011, **133**, 16986–16996.
21. E. Poeselt, S. Fischer, S. Foerster, and H. Weller, *Langmuir*, 2009, **25**, 13906–13913.
22. X. Wang, G. Li, T. Chen, M. Yang, Z. Zhang, T. Wu, and H. Chen, *Nano Lett.*, 2008, **8**, 2643–2647.
23. Y. Mai and A. Eisenberg, *J. Am. Chem. Soc.*, 2010, **132**, 10078–10084.
24. Q. Luo, R. J. Hickey, and S.-J. Park, *ACS Macro Lett.*, 2013, **2**, 107–111.
25. C.-A. J. Lin, R. A. Sperling, J. K. Li, T.-Y. Yang, P.-Y. Li, M. Zanella, W. H. Chang, and W. J. Parak, *Small*, 2008, **4**, 334–341.
26. J. Rodríguez-Fernández, J. Pérez-Juste, F. J. García de Abajo, and L. M. Liz-Marzán, *Langmuir*, 2006, **22**, 7007–7010.
27. M. Liu and P. Guyot-Sionnest, *J. Phys. Chem. B*, 2005, **109**, 22192–22200.
28. H. Yuan, C. G. Khoury, H. Hwang, C. M. Wilson, G. A. Grant, and T. Vo-Dinh, *Nanotechnology*, 2012, **23**, 075102.
29. J. Pérez-Juste, I. Pastoriza-Santos, L. M. Liz-Marzán, and P. Mulvaney, *Coord. Chem. Rev.*, 2005, **249**, 1870–1901.
30. L. M. Liz-Marzán, M. Giersig, and P. Mulvaney, *Langmuir*, 1996, **12**, 4329–4335.
31. R. Contreras-Cáceres, A. Sánchez-Iglesias, M. Karg, I. Pastoriza-Santos, J. Pérez-Juste, J. Pacifico, T. Hellweg, A. Fernández-Barbero, and L. M. Liz-Marzán, *Adv. Mater.*, 2008, **20**, 1666–1670.
32. S. Barbosa, A. Agrawal, L. Rodríguez-Lorenzo, I. Pastoriza-Santos, R. A. Alvarez-Puebla, A. Kornowski, H. Weller, and L. M. Liz-Marzán, *Langmuir*, 2010, **26**, 14943–14950.
33. A. M. Funston, C. Novo, T. J. Davis, and P. Mulvaney, *Nano Lett.*, 2009, **9**, 1651–1658.
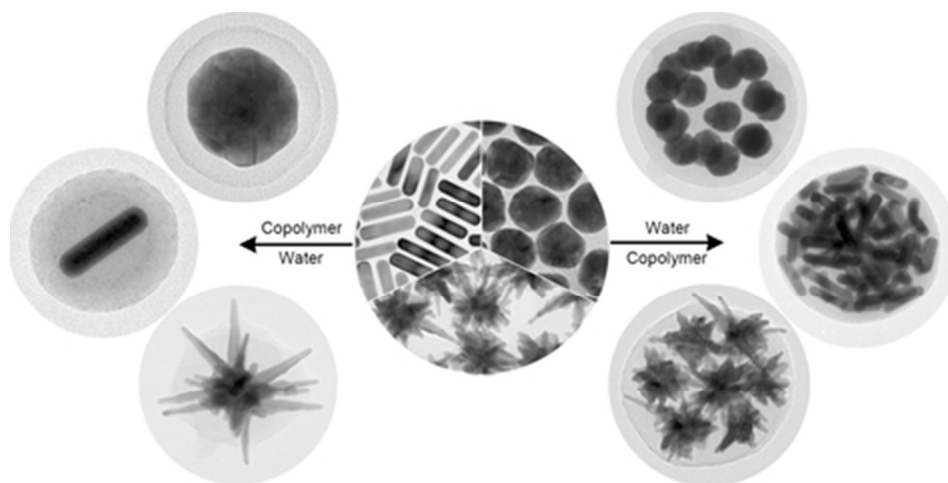
A generic method for the preparation of polymer-coated plasmonic nanostructures with tunable thickness of the hydrophobic polymer spacer.
39x19mm (300 x 300 DPI)